Hydride state accumulation in native [FeFe]-hydrogenase with the physiological reductant H_2 supports its catalytic relevance†

Moritz Senger, *[a] Tobias Kernmayr,[b, ††] Marco Lorenzi,[b] Holly J. Redman[b] and Gustav Berggren*[b]

[a.] *Department of Chemistry, Physical Chemistry, Uppsala University, 75120 Uppsala, Sweden.*

[b.] *Department of Chemistry, Molecular Biomimetics, Uppsala University, 75120 Uppsala, Sweden.*

† Electronic Supplementary Information (ESI) available: Materials and methods, FTIR spectra, Gas interaction kinetics.

†† Current address: Department of Chemistry, Ludwig-Maximilians-Universität München, 81377 München, Germany

Small molecules in solution may affect the stability of catalytic states and produce off-cycle states that can be mistaken for catalytically relevant species. Here we show that the hydride state (Hhyd), a proposed central intermediate in the catalytic cycle of [FeFe] hydrogenase, can be formed in wild-type [FeFe]-hydrogenases treated with H2 in strict absence of other, non-biological, reductants. Moreover, we reveal a new state with unclear role in catalysis induced by common low pH buffers.

Hydrogenases are redox enzymes catalysing molecular hydrogen (H_2) uptake and production. The high H_2 evolution frequency of prototypical [FeFe]-hydrogenases motivates basic research on the reaction mechanism and inspires catalyst design for a hydrogen economy.[1-3] In these enzymes, hydrogen catalysis takes place at a hexa-iron cofactor, called the H-cluster. It is composed of a [4Fe4S]-cluster linked via a cysteine residue to a unique diiron site ([2Fe]) that binds two cyanide (CN^-) and three carbonyl (CO) ligands. These ligands serve as intrinsic probes sensitive to *infrared* spectroscopy and report on reduction and protonation events during catalysis. The diiron site is bridged by an azadithiolate ligand ($^-SCH_2NHCH_2S^-$, ADT) that is proposed to shuttle protons via its amine group to the apical vacancy, the site of hydrogen catalysis, located at the Fe ion (Fe_d) distal to the [4Fe4S] cluster (Fig.1). The most studied group of [FeFe]-hydrogenases (Group A) transfers protons to the active site via a conserved Proton Transfer Pathway (PTP) composed of amino acid residues and water molecules.[4-6] Recently described [FeFe]-hydrogenases in group D lack this PTP.[7, 8] Several redox and protonation states have been characterised and proposed as catalytic intermediates.[1, 2] The starting point of catalysis is the oxidised state Hox. Under oxidising conditions at low pH values and in presence of chemical reductant a blue-shifted variant of Hox is formed, commonly denoted HoxH.[9, 10] One electron reduction of Hox results in population of two singly reduced states: Hred' or Hred. Hred' features a reduced [4Fe4S] cluster while the diiron site is still in an oxidised configuration. Formation of the diiron site reduced state Hred is coupled to a proton uptake event, although the site of protonation is under discussion.[11, 12] A second reduction step yields the super-reduced state (Hsred) or the hydride state (Hhyd). Hsred is characterised by a reduction of both the [4Fe4S] cluster and the diiron site.[13] In contrast, Hhyd features a terminal hydride at Fe_d, yielding a formally oxidized diiron

site (Fig.1).[14-16] As the last step in hydrogen turnover, the terminal hydride of Hhyd is proposed to combine with a proton delivered via the PTP to generate molecular hydrogen.[1-3] A hydride state similar to Hhyd but with an additionally protonated ADT bridge has been proposed as the last intermediate in hydrogen evolution.[17-20] The Hhyd state can be stabilised by amino acid variations in the PTP or cofactor alteration, which has enabled its characterization using a range of techniques, including NMR, Mössbauer, EPR and FTIR spectroscopy.[14-16, 18, 21, 22] In native [FeFe]-hydrogenases the accumulation of Hhyd is commonly achieved by exposure to H_2 at low pH values in the presence of the non-physiological reductant sodium dithionite (NaDT) (with exceptions[23-25]).[16, 19, 22, 26, 27] Therefore, the relevance of Hhyd as a catalytic intermediate could be questioned as a recent study proposed, on the basis of reduced currents in chronoamperometry experiments with sodium sulfite, that [FeFe]-hydrogenases are inhibited by NaDT (or one of its oxidized by-products) at low pH values.[28] Considering its in-depth spectroscopic characterization, and proposed central importance in the catalytic cycle, the possibility that Hhyd represents an inhibited "artefact-state" would represent a significant setback in our mechanistic understanding of [FeFe]-hydrogenase. Here, we selectively enrich the double reduced states, Hhyd and Hsred, by exposure to molecular hydrogen and follow the respective absorbance changes of cofactor ligand bands by Attenuated Total Reflection Fourier-transform *Infrared* (ATR-FTIR) Spectroscopy. Data is collected at different pH values and buffers. This study reveals that small carboxylic acid molecules often used in low pH buffers in enzyme electrochemistry experiments are non-innocent in formation of a new H-cluster species similar to Hox. At present it is not clear if this is an artefactual off-cycle state, or in fact a critical intermediate that previously have escaped detection. Moreover, we show the accumulation of Hhyd in native [FeFe]-hydrogenase, HydA1 from *Chlamydomonas reinhardtii*, at mildly basic and low pH values regardless of buffer choice and more importantly in the *absence* of NaDT. Our findings are well in accordance with Hhyd as a reaction intermediate rather than an experimental artefact.

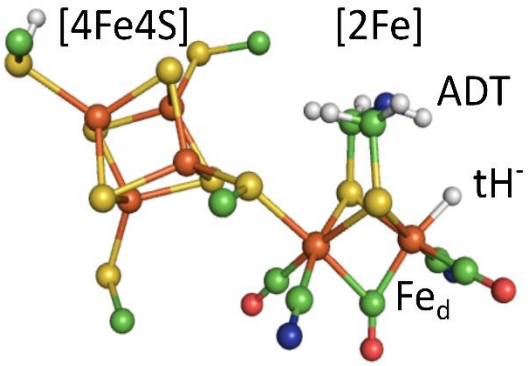

Figure 1 The hydride state of the H-cluster in [FeFe]-hydrogenases. The H-cluster consists of a protein bound [4Fe4S] cluster that is covalently linked via a cysteine thiolate ligand to the diiron site ([2Fe]), further ligated by three carbonyl (CO) and two cyanide (CN^-) ligands. A terminal hydride (tH^-) at the distal iron ion is proposed to combine with a proton delivered by the ADT ligand to yield molecular hydrogen in the last step of hydrogen catalysis. Colour code: orange-iron, yellow-sulphur, green-carbon, red-oxygen, blue-nitrogen, white-hydrogen. The structure is drawn after the PDB coordinates 4XDC optimized for the Hhyd state by DFT calculations.(ref 33)

A NaDT free solution of the HydA1 [FeFe]-hydrogenase was applied to the crystal surface of the ATR-FTIR setup and subsequently dried and rehydrated under N_2 atmosphere to form an auto-oxidised protein film.[29, 30] The hydrogenase adopted the expected oxidised active-ready state Hox, and was subsequently exposed to H_2 gas. The resulting difference spectra are displayed in Figure 2. As a consequence of H_2 uptake, a mixture of the hydride state Hhyd (blue positive bands, 2081, 2066, 1979, 2960, 1860 cm^{-1}) and the super-reduced state Hsred (red positive bands, 2070, 2025, 1954, 1918, 1882 cm^{-1}) was populated while the oxidised state Hox (grey negative bands, 2089, 2071, 1965, 1940, 1802 cm^{-1}) was depopulated. This holds true for different pH values, in a range of different buffers. Figure 2 displays the ATR-FTIR difference spectra of HydA1 samples adjusted to pH 8 or pH 4 and subsequently exposed to H_2 (absolute spectra and pH adjustment in Fig S1). In each spectrum the signature of Hhyd (blue positive bands) is clearly detectable. A larger fraction of Hsred is formed at pH 8 (100 mM Tris buffer) while a larger fraction of Hhyd is populated at pH 4 (100 mM propionate buffer), in both cases a concomitant loss of Hox is observed in contrast to earlier results where a depopulation of HoxH was observed at pH 4 due to the presence of NaDT.[9, 10, 16] However, the preference for Hhyd accumulation at low pH seems to be independent of the presence of NaDT. As Hhyd and Hsred are generally considered to reflect two different tautomers, their relative stability as a function of pH value is arguably influenced by the protonation state of the H-cluster surroundings. The reaction of auto-oxidised HydA1 films with H_2 gas proceeds within 1 second while auto-oxidation, observed when H_2 was replaced by N_2, occurs over 10-20 seconds (compare Fig S2). Both kinetics report indirectly

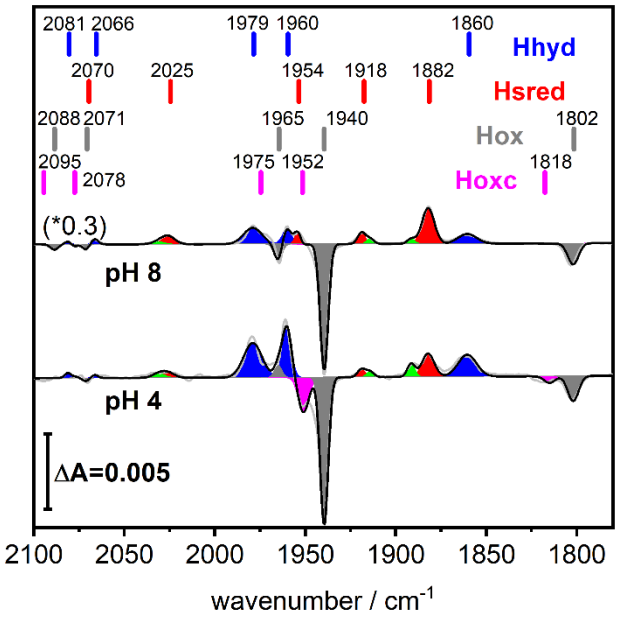

Figure 2 Hydrogen uptake induced ATR-FTIR difference spectra of the CO/CN ligands of HydA1 Upon exposure to H_2 the oxidised state Hox (grey negative bands) is depopulated while double reduced redox states Hsred (red positive bands) and Hhyd (blue positive bands) accumulate. For both pH values, pH 8 (top, 100 mM Tris buffer, scaled by 0.3) and pH 4 (bottom, 100mM propionate buffer), the formation of Hhyd (blue) is observed in the absence of NaDT. Magenta negative bands at 1952 and 1815 cm^{-1} indicate the newly observed, unknown H-cluster species denoted Hoxc. Green bands belong to Hred. The band positions are indicated by bars.

on the gas accessibility and hydration of the protein film in the ATR-FTIR setup. Dehydrated [FeFe]-hydrogenase samples were reported to be protected from exposure to gases.[31]

Figure 2 (bottom) shows that H_2 exposure causes Hhyd accumulation in the absence of NaDT preferentially at low pH values (compare Fig.2 top). This trend had been reported by several groups before, however *always involving* NaDT.[16, 17, 19, 26] Apart from the recent proposed binding of NaDT (or one its oxidized products) to the H-cluster, protonation has been suggested to stabilize the reduction at the [4Fe4S] cluster for Hred'[9, 10, 32] and a similar stabilisation effect was reported for Hhyd from both purely computational and spectroscopic approaches. [33, 34] Our findings verify that NaDT is not required to stabilize Hhyd. The observed pH dependent shift between Hsred and Hhyd instead supports a model of a protonatable, site either near the reduced [4Fe4S] cluster as previously proposed,[3, 32, 35] or e.g. in the PTP. Residual traces of NaDT have been shown to lead to population of HoxH (2089, 2079, 1970, 1945, 1810 cm^{-1})[28], which is absent in our spectra. The negative bands in the pH 4 difference spectrum (Fig.2 bottom) at 1952 and 1815 cm^{-1} belong to an unknown band pattern significantly different from HoxH (full spectroscopic signature Fig.3), and we denote this new state as Hoxc. This blue shifted Hox population was observable with pH 4 buffers composed of formic acid, acetic acid or propionic acid (Fig.3) while usage of larger acids such as succinate or citrate did not induce the new species (Fig.S3).

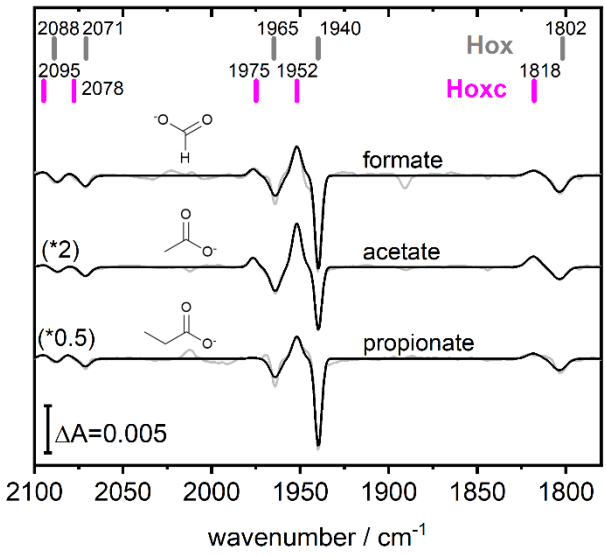

Figure 3 The full spectroscopic signature of Hoxc. Difference spectra highlighting the full band pattern of Hoxc (positive bands) for transitions from pH 8 (10 mM Tris, negative bands) to pH 4 with 100 mM formate (top), 100 mM acetate (middle) and 100 mM propionate (bottom) buffer. Data in grey and fit in black. The band positions are indicated by bars.

Thus, population of the new species, Hoxc, appear to be determined by the size of the carboxylic acid acting as a buffer. Compared to Hox the overall band pattern of Hoxc is retained and in analogy to Hred' (red shifted) and HoxH (blue shifted) we propose that the H-cluster geometry and electronic structure is highly similar. Moreover, the requirement for low pH in forming the state implies that the buffer molecule interacts in its protonated, uncharged, form (Fig.S4). A complete characterisation of this new H-cluster state is beyond the scope of the current study, but we note that it could be of high relevance in particular as e.g. acetic acid (acetate) is commonly employed in protein film electrochemistry studies of [FeFe]-hydrogenase.[23, 28, 36-45] The extent of the new state (Hoxc) formed in electrochemistry setups, its role in catalysis and its implication on catalytic currents, especially at low pH, remain unclear. Low molecular weight carbon-compound binding to Fe_d and inhibitory effects were reported for formaldehyde before.[46-48] However, the Hhyd state forms regardless of the nature of the buffer, rendering a stabilizing role of the buffer molecules unlikely (Fig. 2 and S1). In closing, our data shows clearly that Hhyd can be accumulated in the *absence* of NaDT and without introducing loss-of-function mutations. As a consequence, it is tempting to conclude that Hhyd indeed represents one of the final intermediates in hydrogen evolution catalysis of [FeFe]-hydrogenases.

The authors would like to thank Leif Hammarström for critically reviewing the manuscript. Open access funding was provided by Uppsala University. The European Research Council (ERC, to GB, Contract No. 714102) as well as the European Union's Horizon 2020 research and innovation program (Marie Skłodowska Curie Grant No. 897555 to M.S.) are gratefully acknowledged for funding.

Investigation by M.S. and T.K., M.L. (enzyme purification), H.J.R. (cofactor synthesis), writing (original draft) by M.S., writing (review & editing) M.S., T.K., M.L., H.J.R. and G.B.

There are no conflicts to declare.

Notes and References

1. J. T. Kleinhaus, F. Wittkamp, S. Yadav, D. Siegmund and U. P. Apfel, *Chem Soc Rev*, 2021, **50**, 1668-1784.
2. H. Land, M. Senger, G. Berggren and S. T. Stripp, *Acs Catal*, 2020, **10**, 7069-7086.
3. F. Wittkamp, M. Senger, S. T. Stripp and U. P. Apfel, *Chem Commun (Camb)*, 2018, **54**, 5934-5942.
4. M. Winkler, J. Esselborn and T. Happe, *Biochim Biophys Acta*, 2013, **1827**, 974-985.
5. J. Duan, M. Senger, J. Esselborn, V. Engelbrecht, F. Wittkamp, U. P. Apfel, E. Hofmann, S. T. Stripp, T. Happe and M. Winkler, *Nat Commun*, 2018, **9**, 4726.
6. M. Senger, V. Eichmann, K. Laun, J. Duan, F. Wittkamp, G. Knor, U. P. Apfel, T. Happe, M. Winkler, J. Heberle and S. T. Stripp, *J Am Chem Soc*, 2019, **141**, 17394-17403.
7. H. Land, A. Sekretareva, P. Huang, H. J. Redman, B. Nemeth, N. Polidori, L. S. Meszaros, M. Senger, S. T. Stripp and G. Berggren, *Chem Sci*, 2020, **11**, 12789-12801.
8. H. Land, P. Ceccaldi, L. S. Meszaros, M. Lorenzi, H. J. Redman, M. Senger, S. T. Stripp and G. Berggren, *Chem Sci*, 2019, **10**, 9941-9948.
9. M. Senger, K. Laun, F. Wittkamp, J. Duan, M. Haumann, T. Happe, M. Winkler, U. P. Apfel and S. T. Stripp, *Angew Chem Int Ed Engl*, 2017, **56**, 16503-16506.
10. M. Senger, S. Mebs, J. Duan, O. Shulenina, K. Laun, L. Kertess, F. Wittkamp, U. P. Apfel, T. Happe, M. Winkler, M. Haumann and S. T. Stripp, *Phys Chem Chem Phys*, 2018, **20**, 3128-3140.
11. S. Mebs, M. Senger, J. Duan, F. Wittkamp, U. P. Apfel, T. Happe, M. Winkler, S. T. Stripp and M. Haumann, *J Am Chem Soc*, 2017, **139**, 12157-12160.
12. C. Sommer, A. Adamska-Venkatesh, K. Pawlak, J. A. Birrell, O. Rudiger, E. J. Reijerse and W. Lubitz, *J Am Chem Soc*, 2017, **139**, 1440-1443.
13. A. Silakov, C. Kamp, E. Reijerse, T. Happe and W. Lubitz, *Biochemistry-Us*, 2009, **48**, 7780-7786.
14. D. W. Mulder, Y. Guo, M. W. Ratzloff and P. W. King, *J Am Chem Soc*, 2017, **139**, 83-86.

15. E. J. Reijerse, C. C. Pham, V. Pelmenschikov, R. Gilbert-Wilson, A. Adamska-Venkatesh, J. F. Siebel, L. B. Gee, Y. Yoda, K. Tamasaku, W. Lubitz, T. B. Rauchfuss and S. P. Cramer, *J Am Chem Soc*, 2017, **139**, 4306-4309.
16. M. Winkler, M. Senger, J. Duan, J. Esselborn, F. Wittkamp, E. Hofmann, U. P. Apfel, S. T. Stripp and T. Happe, *Nat Commun*, 2017, **8**, 16115.
17. D. W. Mulder, M. W. Ratzloff, E. M. Shepard, A. S. Byer, S. M. Noone, J. W. Peters, J. B. Broderick and P. W. King, *J Am Chem Soc*, 2013, **135**, 6921-6929.
18. D. W. Mulder, M. W. Ratzloff, M. Bruschi, C. Greco, E. Koonce, J. W. Peters and P. W. King, *J Am Chem Soc*, 2014, **136**, 15394-15402.
19. L. S. Meszaros, P. Ceccaldi, M. Lorenzi, H. J. Redman, E. Pfitzner, J. Heberle, M. Senger, S. T. Stripp and G. Berggren, *Chem Sci*, 2020, **11**, 4608-4617.
20. A. Adamska, A. Silakov, C. Lambertz, O. Rudiger, T. Happe, E. Reijerse and W. Lubitz, *Angew Chem Int Ed Engl*, 2012, **51**, 11458-11462.
21. P. Knorzer, A. Silakov, C. E. Foster, F. A. Armstrong, W. Lubitz and T. Happe, *J Biol Chem*, 2012, **287**, 1489-1499.
22. M. W. Ratzloff, J. H. Artz, D. W. Mulder, R. T. Collins, T. E. Furtak and P. W. King, *J Am Chem Soc*, 2018, **140**, 7623-7628.
23. P. Rodríguez-Maciá, N. Breuer, S. DeBeer and J. A. Birrell, *Acs Catal*, 2020, **10**, 13084-13095.
24. S. Morra, J. Duan, M. Winkler, P. A. Ash, T. Happe and K. A. Vincent, *Dalton Trans*, 2021, **50**, 12655-12663.
25. P. S. Corrigan, J. L. Tirsch and A. Silakov, *J Am Chem Soc*, 2020, **142**, 12409-12419.
26. C. Lorent, S. Katz, J. Duan, C. J. Kulka, G. Caserta, C. Teutloff, S. Yadav, U. P. Apfel, M. Winkler, T. Happe, M. Horch and I. Zebger, *J Am Chem Soc*, 2020, **142**, 5493-5497.
27. V. Pelmenschikov, J. A. Birrell, C. C. Pham, N. Mishra, H. Wang, C. Sommer, E. Reijerse, C. P. Richers, K. Tamasaku, Y. Yoda, T. B. Rauchfuss, W. Lubitz and S. P. Cramer, *J Am Chem Soc*, 2017, **139**, 16894-16902.
28. M. A. Martini, O. Rudiger, N. Breuer, B. Noring, S. DeBeer, P. Rodriguez-Macia and J. A. Birrell, *J Am Chem Soc*, 2021, **143**, 18159-18171.
29. M. Senger, S. Mebs, J. Duan, F. Wittkamp, U. P. Apfel, J. Heberle, M. Haumann and S. T. Stripp, *Proc Natl Acad Sci U S A*, 2016, **113**, 8454-8459.
30. S. T. Stripp, *Acs Catal*, 2021, **11**, 7845-7862.
31. J. Noth, R. Kositzki, K. Klein, M. Winkler, M. Haumann and T. Happe, *Sci Rep*, 2015, **5**, 13978.
32. K. Laun, I. Baranova, J. Duan, L. Kertess, F. Wittkamp, U. P. Apfel, T. Happe, M. Senger and S. T. Stripp, *Dalton Trans*, 2021, **50**, 3641-3650.
33. P. E. M. Siegbahn and R. Z. Liao, *J Phys Chem A*, 2020, **124**, 10540-10549.

34. S. Mebs, R. Kositzki, J. Duan, L. Kertess, M. Senger, F. Wittkamp, U. P. Apfel, T. Happe, S. T. Stripp, M. Winkler and M. Haumann, *Biochim Biophys Acta Bioenerg*, 2018, **1859**, 28-41.
35. M. Haumann and S. T. Stripp, *Acc Chem Res*, 2018, **51**, 1755-1763.
36. P. Rodriguez-Macia, L. Kertess, J. Burnik, J. A. Birrell, E. Hofmann, W. Lubitz, T. Happe and O. Rudiger, *J Am Chem Soc*, 2019, **141**, 472-481.
37. O. Lampret, A. Adamska-Venkatesh, H. Konegger, F. Wittkamp, U. P. Apfel, E. J. Reijerse, W. Lubitz, O. Rudiger, T. Happe and M. Winkler, *J Am Chem Soc*, 2017, **139**, 18222-18230.
38. L. Kertess, F. Wittkamp, C. Sommer, J. Esselborn, O. Rudiger, E. J. Reijerse, E. Hofmann, W. Lubitz, M. Winkler, T. Happe and U. P. Apfel, *Dalton Trans*, 2017, **46**, 16947-16958.
39. L. Kertess, A. Adamska-Venkatesh, P. Rodriguez-Macia, O. Rudiger, W. Lubitz and T. Happe, *Chem Sci*, 2017, **8**, 8127-8137.
40. O. Lampret, J. Duan, E. Hofmann, M. Winkler, F. A. Armstrong and T. Happe, *Proc Natl Acad Sci U S A*, 2020, **117**, 20520-20529.
41. V. Hajj, C. Baffert, K. Sybirna, I. Meynial-Salles, P. Soucaille, H. Bottin, V. Fourmond and C. Leger, *Energ Environ Sci*, 2014, **7**, 715-719.
42. M. Del Barrio, M. Sensi, L. Fradale, M. Bruschi, C. Greco, L. de Gioia, L. Bertini, V. Fourmond and C. Leger, *J Am Chem Soc*, 2018, **140**, 5485-5492.
43. M. Winkler, J. Duan, A. Rutz, C. Felbek, L. Scholtysek, O. Lampret, J. Jaenecke, U. P. Apfel, G. Gilardi, F. Valetti, V. Fourmond, E. Hofmann, C. Leger and T. Happe, *Nat Commun*, 2021, **12**, 756.
44. S. Hardt, S. Stapf, D. T. Filmon, J. A. Birrell, O. Rudiger, V. Fourmond, C. Leger and N. Plumere, *Nat Catal*, 2021, **4**, 251-258.
45. A. Fasano, H. Land, V. Fourmond, G. Berggren and C. Leger, *J Am Chem Soc*, 2021, DOI: 10.1021/jacs.1c09554.
46. A. F. Wait, C. Brandmayr, S. T. Stripp, C. Cavazza, J. C. Fontecilla-Camps, T. Happe and F. A. Armstrong, *J Am Chem Soc*, 2011, **133**, 1282-1285.
47. C. E. Foster, T. Kramer, A. F. Wait, A. Parkin, D. P. Jennings, T. Happe, J. E. McGrady and F. A. Armstrong, *J Am Chem Soc*, 2012, **134**, 7553-7557.
48. F. Zhang, T. J. Woods, L. Zhu and T. B. Rauchfuss, *Chem Sci*, 2021, **12**, 15673-15681.

Supporting Information

Hydride state accumulation in native [FeFe]-hydrogenase with the physiological reductant H_2 supports its catalytic relevance†

Moritz Senger,*[a] Tobias Kernmayr,[b, ††] Marco Lorenzi,[b] Holly J. Redman[b] and Gustav Berggren*[b]

a) Department of Chemistry, Physical Chemistry, Uppsala University, 75120 Uppsala, Sweden

b) Department of Chemistry, Molecular Biomimetics, Uppsala University, 75120 Uppsala, Sweden

††) Current address: Department of Chemistry, Ludwig-Maximilians-Universität München, 81377 München, Germany

Materials and Methods:

Protein purification and the absence of NaDT *Chlamydomonas reinhardtii* HydA1 was expressed, purified and reconstituted with minor modifications as previously reported.[1, 2] The codon-optimized gene coding for *Cr*HydA1 was cloned in frame with a Strep-tag II on a pET11a vector by GeneScript, that was then used BL21(DE3) E. coli strain. The enzyme was aerobically expressed in its *apo*-form and purified using pre-packed StrepTrap columns on an Äkta-Ready system (Cytiva). After semi-enzymatic [4Fe4S] cluster reconstitution, the enzyme was matured using a $Fe_2(adt)(CO)_4(CN)_2^{2-}$ (adt = azadithiolate, $^{-}SCH_2NHCH_2S^{-}$) synthetic mimic as follows: a mixture containing 100uM reconstituted *Cr*HydA1, 600uM $Fe_2(adt)(CO)_4(CN)_2^{2-}$, 2mM sodium dithionite was prepared in a 100mM Tris/HCl pH 8, 200mM KCl buffer; the mixture was incubated for 90 minutes at room temperature and excess mimic and dithionite were removed using a PD10 desalting column, pre-equilibrated with a 100mM Tris/HCl pH 8, 200mM KCl buffer. To ensure complete removal of residual dithionite, the buffer was further exchanged to 10mM Tris/HCl pH 8 via four concentration and dilution cycles using Amicon® Ultra 0.5 Centrifugal Filter Units (Millipore), as recommended by the manufacturer.

ATR-FTIR spectroscopy 1µl enzyme solution (1mM CrHydA1) in 10 mM Tris buffer (pH 8) was deposited on the ATR crystal in the anaerobic atmosphere of a Braun Glove box. The ATR unit (BioRadII from Harrick) was sealed with a custom build PEEK cell that allowed for gas exchange and illumination (inspired by Stripp et al.[3, 4]) mounted in a FTIR spectrometer (Vertex V70v, Bruker). The sample was dried under 100% nitrogen gas and rehydrated with a humidified aerosol (100 mM Tris-HCl (pH 8) or 100 mM propionate/acetate/formate buffer (pH 4)) as described before[5]. Spectra were recorded with 2 cm^{-1} resolution, a scanner velocity of 80 Hz and averaged of varying number of scans (mostly 1000 Scans). All measurements were performed at ambient conditions (room temperature and pressure, hydrated enzyme films).

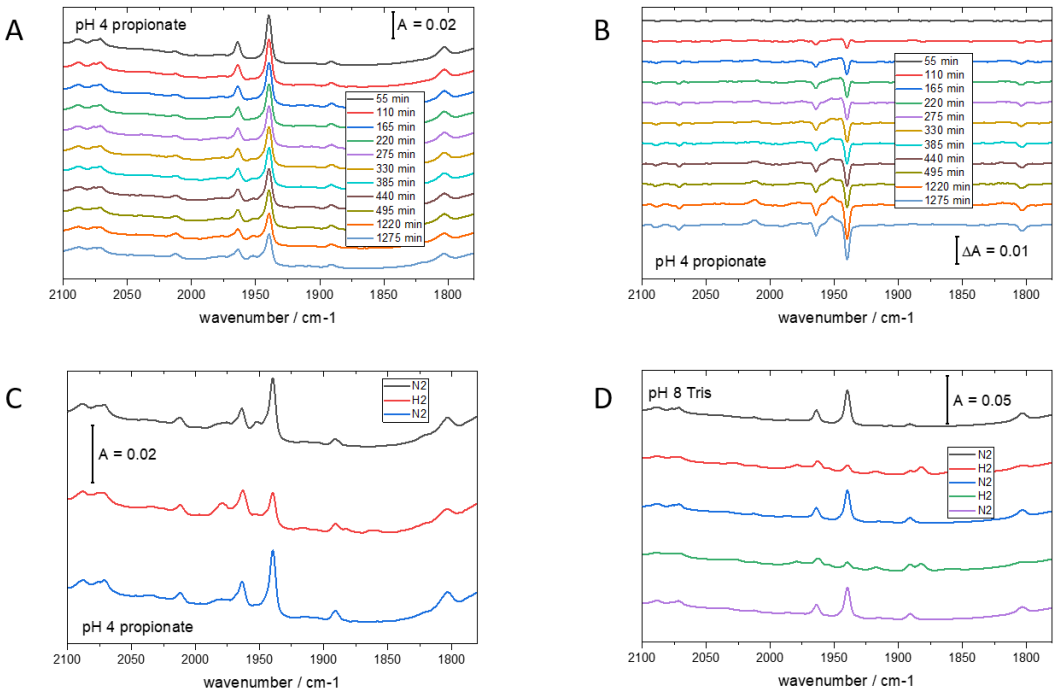

Figure S1 Absolute and difference ATR-FTIR spectra of HydA1 during the pH 4 adjustment and under H_2 and N_2. (A) Absolute spectra of HydA1 (10mM Tris pH 8) exposed to a 100 mM propionate buffer (pH 4) via the aerosol. Formation of the new species Hoxc is followed over time. **(B)** Difference spectra of the same process as in (A). **(C)** Absolute spectra of HydA1 equilibrated at pH 4 (100mM propionate, compare (A) and (B)) exposed to H_2 and N_2. **(D)** Absolute spectra of HydA1 at pH 8 (100 mM Tris) exposed to H_2 and N_2. All spectra read from top to bottom

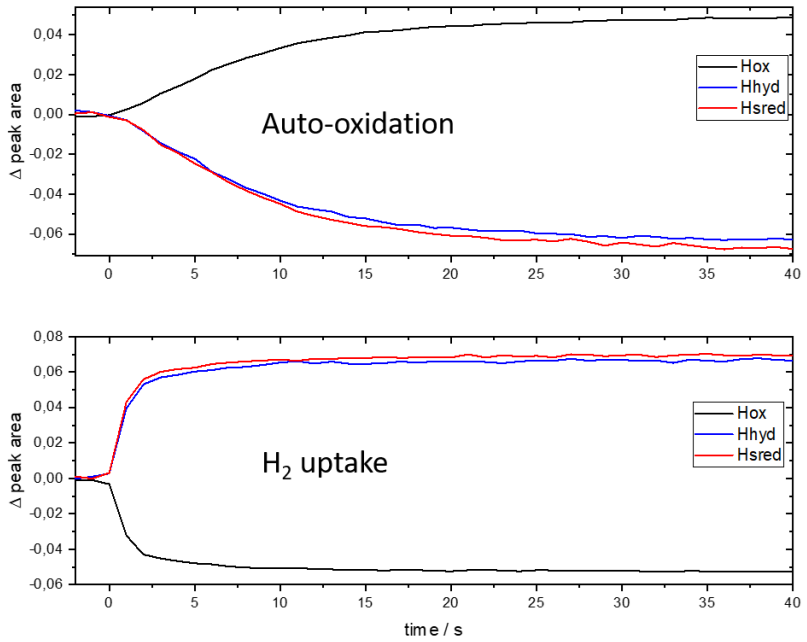

Figure S2 Gas interaction kinetics of HydA1 at pH 4. Plotted is the difference in peak area associated with each redox state over time. Hox is scaled by 0.5. **top:** The sample exposed to N_2 after being equilibrated under H_2 (compare Fig.S1 C) adjusts to the new gas atmosphere (auto-oxidation) within ca. 20 seconds. **bottom:** The sample exposed to H_2 after being equilibrated under N_2 (compare Fig.S1 C) adjusts to the new gas atmosphere (H_2 uptake) within ca. 2 seconds.

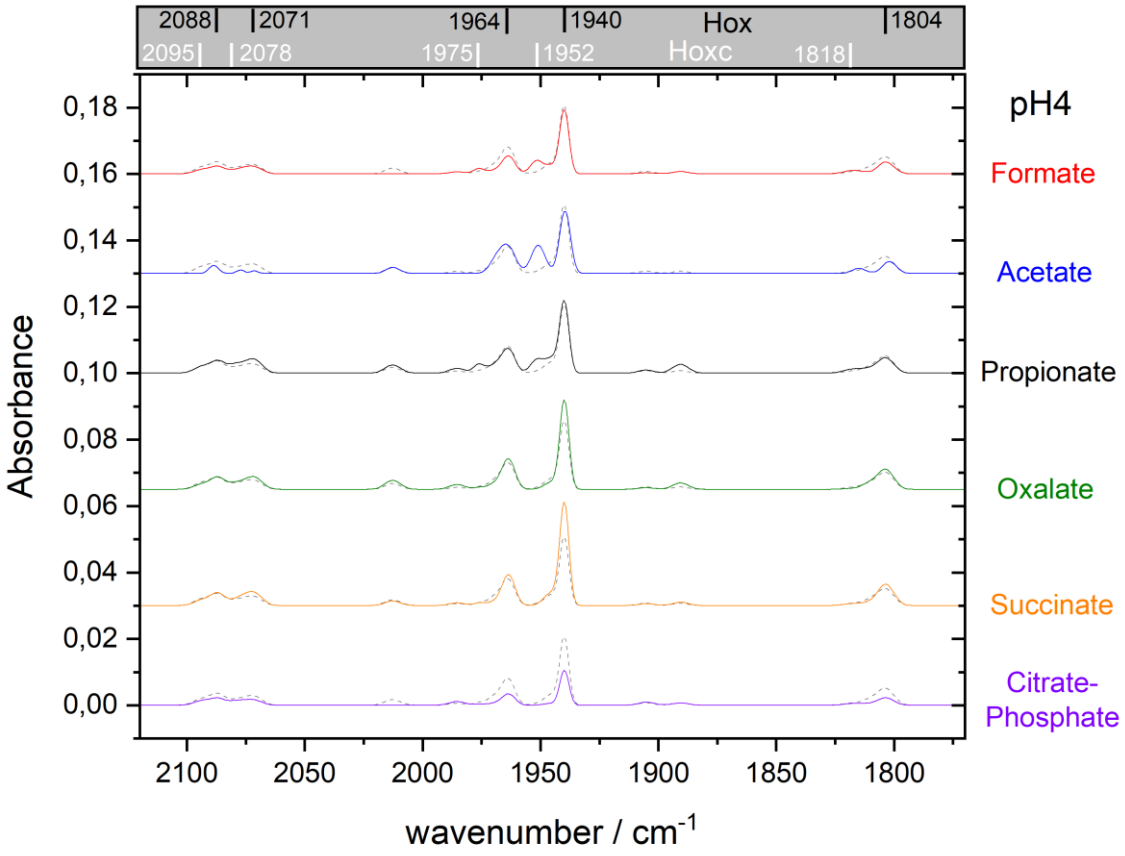

Figure S3 Absolute ATR-FTIR spectra of HydA1 exposed to different buffers. HydA1 exposed to different pH 4 buffers (100 mM) composed of (formate, acetate, propionate, oxalate, succinate, citrate-phosphate). Only for acetate, propionate and formate population of Hoxc is observed. The dashed spectra represent HydA1 at pH 8 (100 mM Tris).

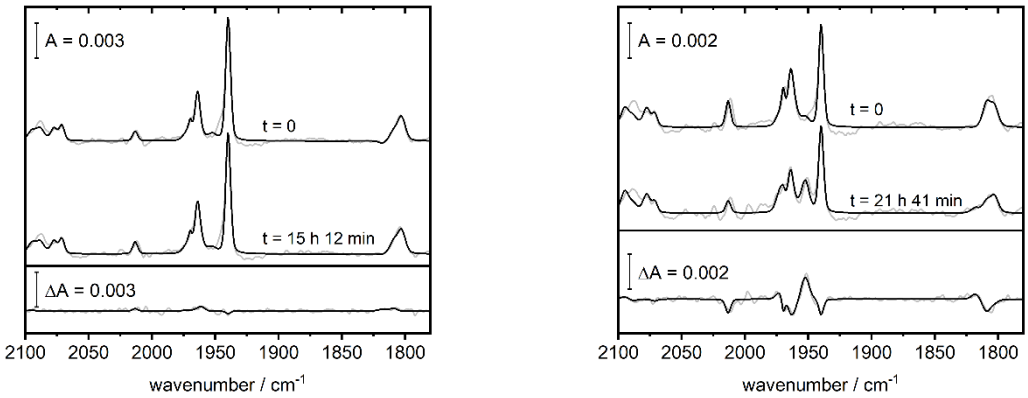

Figure S4 Absolute and difference ATR-FTIR spectra of HydA1 equilibrated with mixed buffer at pH 8 and pH 4. HydA1 exposed to pH 8 and pH 4 with the same buffer composed of 100 mM acetate and 100 mM Tris. The left panel shows the absolute spectra of HydA1 before (t=0) and after (15h 12min) exposure to mixed pH8 buffer. The difference spectrum in the bottom shows that no Hoxc species is formed. The right panel displays the same experiment conducted with mixed buffer at pH 4. The absolute and the difference spectrum show a clear population of Hoxc (21 h 41 min). Grey lines represent the data and black lines the fit.

References:

1. D. W. Mulder, D. O. Ortillo, D. J. Gardenghi, A. V. Naumov, S. S. Ruebush, R. K. Szilagyi, B. Huynh, J. B. Broderick and J. W. Peters, Biochemistry-Us, 2009, 48, 6240-6248.

2. L. S. Meszaros, B. Nemeth, C. Esmieu, P. Ceccaldi and G. Berggren, Angew Chem Int Ed Engl, 2018, 57, 2596-2599.

3. S. T. Stripp, Acs Catal, 2021, 11, 7845-7862.

4. M. Senger, S. Mebs, J. Duan, F. Wittkamp, U. P. Apfel, J. Heberle, M. Haumann and S. T. Stripp, Proc Natl Acad Sci U S A, 2016, 113, 8454-8459.

5. M. Senger, S. Mebs, J. Duan, O. Shulenina, K. Laun, L. Kertess, F. Wittkamp, U. P. Apfel, T. Happe, M. Winkler, M. Haumann and S. T. Stripp, Phys Chem Chem Phys, 2018, 20, 3128-3140.